

## Scientific accomplishments 2020

During 2020 a systematic study started on a serie of Si diodes processed on defect engineered Si, obtained by epitaxial growth of a 45  $\mu\text{m}$  thick layer of Si on 10  $\Omega\text{cm}$  Cz substrates. The growth of all of the epilayers was performed by ITME Warsaw. The only varying parameter imposed for the present study was the amount of incorporated Boron doping. Then the EPI diodes have been produced all by CiS, Germany using the same procedures of implant and processing. This way diodes of different resistivities were obtained, of 10, 50, 250 and 1000  $\Omega\text{cm}$ , all having the same amount of different than Boron impurities (C and O). In the same processing runs CiS produced for the present study also CZ and FZ diodes of 100 and 1000  $\Omega\text{cm}$  resistivity, respectively, to be studied in comparison with EPI diodes. Pairs of diodes from the same wafers were subjected to irradiation with 23 GeV protons and 1 MeV neutrons, fluences between  $10^{10}$  and  $10^{13}$   $\text{cm}^{-2}$  for DLTS investigations and of  $10^{17}$  and  $10^{19}$   $\text{cm}^{-2}$  for TEM investigations.

By using same vendors and processing of all diodes while performing *all the experiments in same place, with the same set-up/procedures* the performed study becomes relevant for understanding the reasons behind the large scattering in the results reported previously for acceptor removal rates in p type Si, by different research groups.

The main results obtained in 2020, according to the type of investigation performed are:

1) Analyses of impurity content. Unirradiated samples were first investigated by spectroscopic techniques in order to determine the amount of C, O and B in the investigated diodes. In Fig. 1 are given the results of SIMS measurements. The amount of C in EPI and CZ materials is  $\sim 1.3 \times 10^{16}$   $\text{cm}^{-3}$  and in FZ is close to the detection limit  $\sim 10^{15}$   $\text{cm}^{-3}$ . The B content could be detected by SIMS only in the low resistivity CZ substrate of the epilayers, in the order of  $2 \times 10^{18}$   $\text{cm}^{-3}$ . By the use of the newly installed LA-ICPMS in NIMP it became possible to detect B in concentration of  $10^{13}$   $\text{cm}^{-3}$ , however, only after developing proper calibration standars.

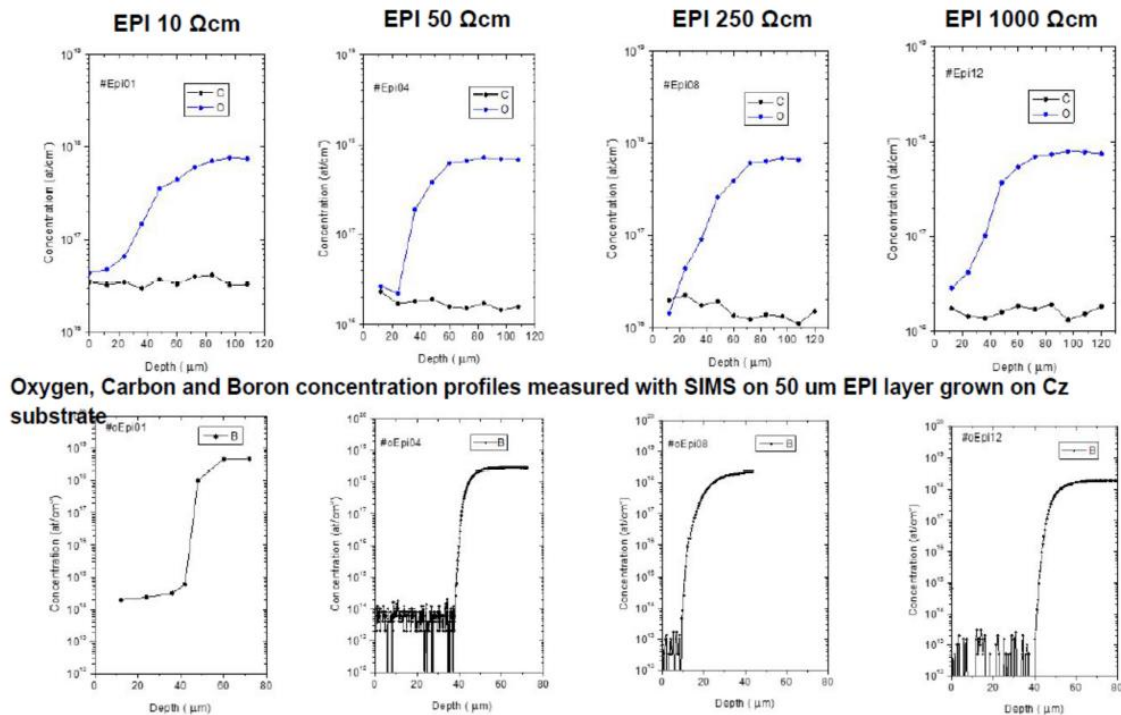


Fig.1. Concentration of C, O and B as detected by SIMS in EPI diodes (45  $\mu\text{m}$  thick epilayers of different resistivities grown on 10  $\Omega\text{cm}$  CZ substrates).

2) TEM investigations – annealing at 80 C. For microstructural investigations the JEOL 2100 TEM has been used. Sample has been prepared using the conventional cross-section method based on mechanical thinning and Ar ion polishing. Point defects have been observed (inset of Fig2a for a 1MeV neutron irradiated LGAD, fluence  $10^{19}$   $\text{cm}^{-2}$ ) and seem to group along tracks normal to the film plane, which is also the neutron irradiation direction.

Strain maps (Fig.2b) have been obtained from HRTEM images as mappings of local displacements of the crystal structure relative to a reference area. The displacements are obtained under the infinitesimal strain assumption, therefore the strain components in the images above can be interpreted as displacements along and normal to the interface ( $\epsilon_{xx}, \epsilon_{yy}$ ) and shear displacements ( $\epsilon_{xy}, \epsilon_{yx}$ ). The magnitude of the strain (max 0,2%) is very low and can be concluded that the structures have no significant internal stress due to the formation of various defects. No changes are observed during the long-term annealing at 80 C.

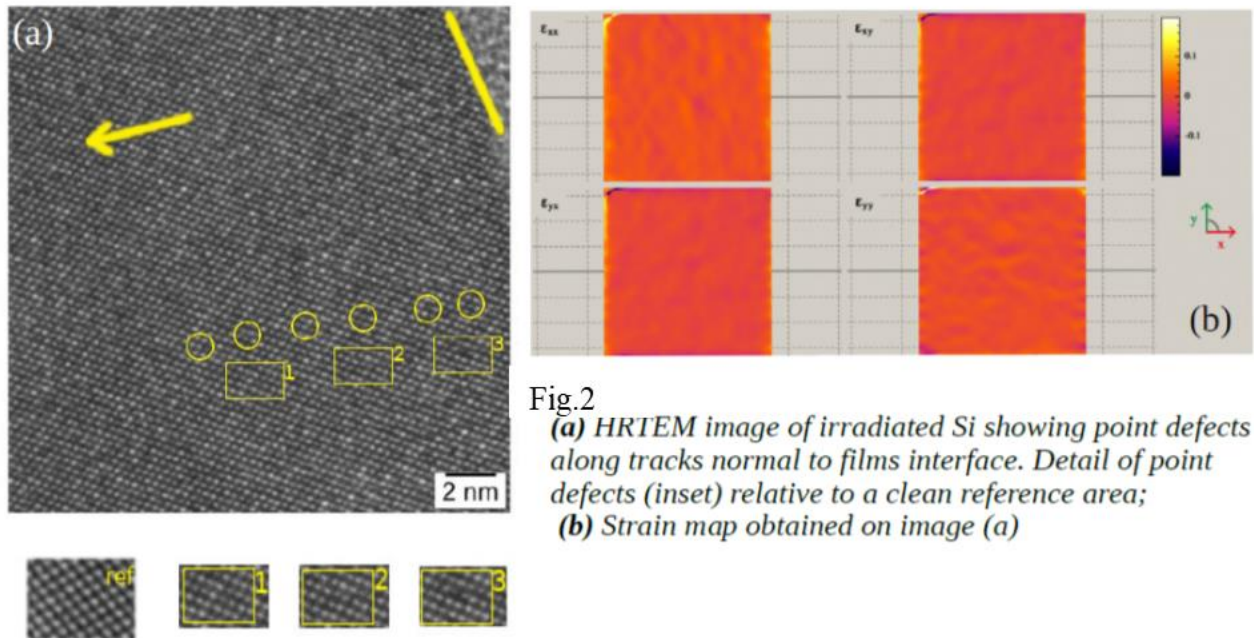


Fig.2  
**(a)** HRTEM image of irradiated Si showing point defects along tracks normal to films interface. Detail of point defects (inset) relative to a clean reference area;  
**(b)** Strain map obtained on image (a)

3) **DLTS investigations:** *detection and electrical characterization of all the defects induced by irradiation, determine the defect generation rate(s) and the role of impurities in their formation, evaluate the impact on the acceptor removal rate (e.g.  $\text{BiO}_i$  defect), time evolution.*

- Four new detected defects acting as traps of holes. Among them only 2 could be well separated and characterized: H156K ( $\sigma_h = 4.8 \times 10^{-16} \text{ cm}^2$  and  $E_a = 0.29 \text{ eV}$ ) and H223K ( $\sigma_h = 1.7 \times 10^{-17} \text{ cm}^2$  and  $E_a = 0.36 \text{ eV}$ ). Characterizing the other 2 defects the DLTS upgrade should be completed.

- *Electrical properties of the  $\text{BiO}_i$  defect, field dependent  $E_a$  and determination of both capture cross sections for electrons and holes ( $E_a = 0.24\text{-}0.25 \text{ eV}$ ,  $\sigma_e = 1 \times 10^{-14} \text{ cm}^2$  and  $\sigma_h = 2.5 \times 10^{-20} \text{ cm}^2$ ). Impact on the device performance: It contributes in full concentration with positive charge to  $N_{\text{eff}}$  at RT and has an insignificant contribution to LC at RT ( $\sim 0.002\% \text{ LC}$ ).*

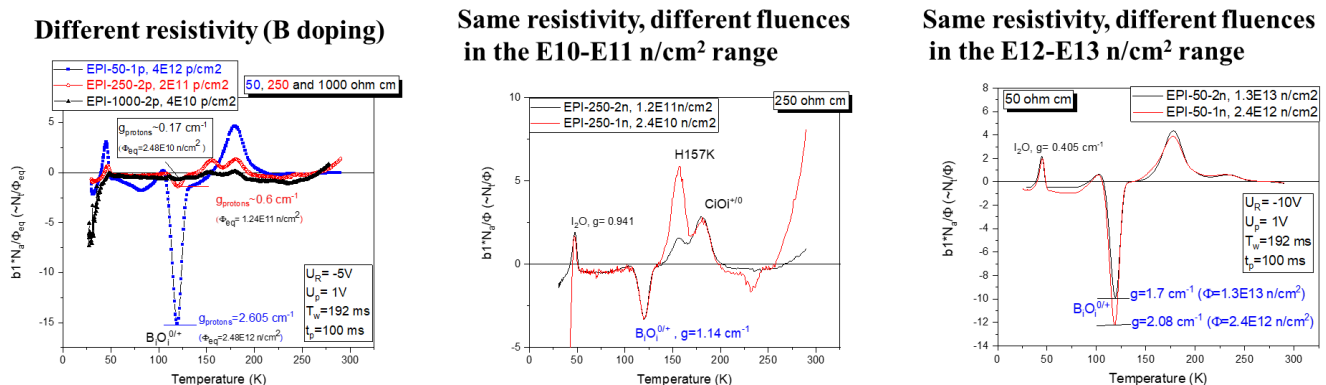


Fig. 3.  $\text{BiO}_i$  generation rate in EPI diodes of different resistivities, exposed to different hadron irradiation (23 GeV protons and 1 MeV neutrons) and different fluences.

- *BiOi defect generation rate(s)*. Our study revealed that the BiOi generation rate does not depend only on B, C and O content but also on the type of irradiation (neutrons or protons) and irradiation fluence. For the same material, same doping and impurity content, the BiOi generation rate stays constant only for low hadron fluence, below  $10^{11} \text{ cm}^{-2}$ . Few examples of the determined BiOi generation rates are given in Fig. 3 for EPI diodes, the measured DLTS signal being depicted in such a way that the BiOi generation rates can be directly compared. Figures 4 and 5 show the dependence of BiOi generation rate on the doping, fluence, type of irradiation and irradiated material. The results show that the rate of BiOi defect generation increases when the resistivity is lowered (as expected), is constant for medium resistivity and fluences below  $E11 \text{ p/cm}^2$  and decreases with increasing the fluence above  $10^{12} \text{ n/cm}^2$ .

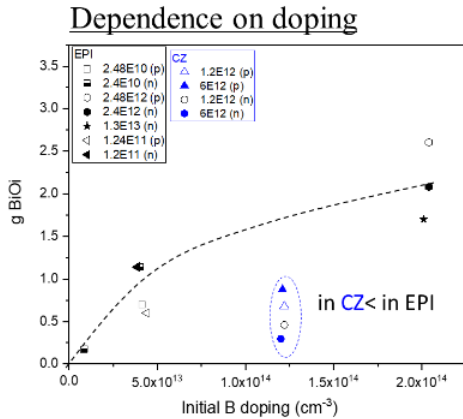


Fig.4. Dependence of BiOi generation rate on B content in EPI diodes – comparison with CZ material.

Dependence on the material (different O content in EPI and CZ materials, similar C content)

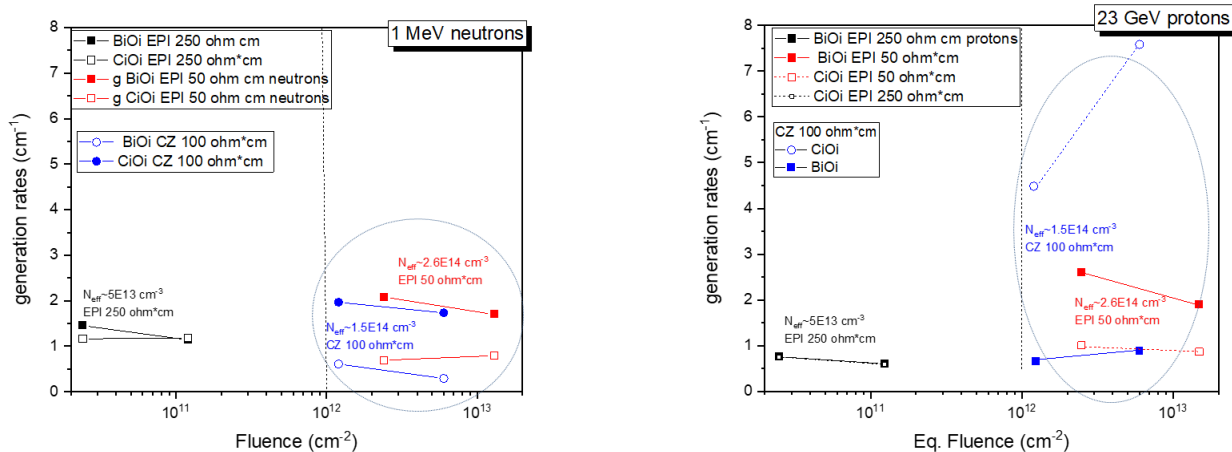


Fig. 5. BiOi and CiOi generation rates in EPI and CZ diodes, for neutron and proton irradiation.

In the same time irradiation with protons induces *more* defects than that with neutrons in low resistivity EPI diodes and *less* in medium and high resistivity ones. The fluence dependence of BiOi in low resistivity CZ material is similar with that of EPI diodes after neutron irradiation but not after proton irradiation. Although the C content in both EPI and CZ diodes is similar, only the O content differs (40 times more in Cz than in EPI), the results cannot be explained accounting for the competing reaction between B and C only. In addition, large scattering of the data exists even for the diodes of the present study for which a lot of precautions were taken (same vendors, same processing, same measurement set-ups and procedures). All together, the results suggest that, beside the known competing reaction generating CiOi defect, at least one another competing mechanism is influencing the generation of BiOi defect and so the acceptor removal rate in p-type Si diodes. It concerns the involving of interstitials in other defects (as e.g. the  $I_2O$  defect, more generated in CZ material). The impact of this defect can be proper evaluated by studying its dissociation at temperatures above 100 C. So far, our annealing studies were performed at  $60^{\circ}C$  and for this temperature the only variation in defect concentration was detected for the  $V_3$  defect which change its configuration from one generating leakage current to another with no impact on the device characteristics.